CROSSED-PLANE IMAGING OF PREMIXED TURBULENT COMBUSTION PROCESSES

F. C. Gouldin
Mechanical and Aerospace Engineering
Cornell University, Ithaca, NY 14853

ABSTRACT

During the last several years we have developed and applied advanced imaging methods – crossed-plane laser tomography and crossed-plane laser Rayleigh imaging -- for high-resolution studies of scalar fields in premixed combustion. Laser tomography with micron sized, silicone oil droplets marks 650 K isothermal surfaces, and we have used crossed-plane tomography to measure for the first time in three dimensions the instantaneous orientation of these surfaces and to determine the probability density function of the surface normal vector, a statistical measure of surface wrinkling. Rayleigh scattering from premixed flames can be used for temperature imaging, and we have developed crossed-plane Rayleigh imaging in order to measure with high-resolution instantaneous temperature fields, temperature gradient vectors and isothermal surface densities in premixed reacting flows. Most recently we have combined crossed-plane tomography with stereo particle image velocimetry to measure for the first time reactant flow velocities and the components of this velocity both perpendicular and tangent to the reaction sheet. In this report progress from the inception of Grant number DAAD 19-99-1-0324 is summarized, and relevant information regarding publications and participants in the research is presented.

TABLE OF CONTENTS

1. Introduction

Premixed turbulent combustion is important in a number of practical devices including spark ignition engines and certain gas turbine combustors. To improve the performance of these engines, e.g., reduce pollutant emissions, and to reduce design time and costs improved models of and design tools for premixed combustion processes are needed. There are a number of important quantities for which models are needed including measures of local mean, chemical reaction rates and their volume integrals.

For a broad range of premixed combustion conditions, the fuel-consuming, heat-releasing chemical reactions are confined to thin sheets distributed, on average, over some finite spatial volume typically referred to as the flame brush. These sheets are characterized chiefly by their local instantaneous structure – the instantaneous spatial distributions of temperature and composition -- their local orientation in space and by their distribution in space over the flame brush. For low to moderate levels of turbulence the local instantaneous structure of these sheets is very similar to that of a premixed laminar flame subject to perturbation by curvature and imposed flow strain, stretch effects.

As turbulence levels increase perturbations of the reaction sheets increase and the similarity to stretched laminar flames diminishes. Several different regimes of premixed turbulent combustion have been identified and are associated with different reaction sheet structures. The number, character, and boundaries between these regimes are still the subject of research, and several different diagrams defining the regimes have been proposed. For discussion, the regime diagram of Peters [1] is presented in Figure 1. The parameters of this diagram are the turbulent intensity, u', the turbulent Reynolds number, Re, the turbulent integral scale, l, the unstretched laminar flame thickness, l_F, the unstretched laminar burning velocity, S_L^0, and two Karlovitz numbers, one based on l_F and the other on the chemical reaction sheet thickness, l_δ. It is important to note that all turbulence properties are defined by conditions in the reactants, a general practice, and that the flame length scales are proportional to the reactant species diffusivity. These facts and the effects of intermittency mean that the boundaries of these regime diagrams are qualitative and not quantitative.

For the wrinkled and corrugated flame regimes (the flamelet regimes) and for at least a portion of the thin reaction zones regime the rate of chemical reaction can be expressed as the product of the area of the reaction sheet and the reaction rate per unit sheet area. Specifically for the mean rate of product formation, <w>, one may write [e.g., 1-3]

$$< w >= \rho_r S_L^0 I_0 \Sigma \qquad (1)$$

ρ_r is the reactant mixture density; S_L^0 is the unstretched laminar flame burning velocity (introduced above); I_0 accounts for the effects of reaction sheet/flamelet stretch and of unsteady flow on the mean burning rate of the reaction sheet; and Σ is the mean reaction sheet surface to volume ratio or the surface density. For Equation 1 to be of practical value one must be able to define 1) a surface (e.g., an isothermal surface) for which Σ can be determined and 2) a mean rate of product formation per unit area of that surface, $\rho_r S_L^0 I_0$. For an unstretched flamelet these steps are straightforward. Just about any isothermal surface, other than those near the hot and cold boundaries of the flamelet, can

be used since these surfaces are locally parallel to each other and the local burning rate is just $\rho_r S_L^0$. As turbulence levels increase, it becomes increasingly difficult to define the surface since fewer and fewer isoscalar surfaces are locally parallel and the definition for the average burning rate per unit surface area becomes correspondingly ambiguous.
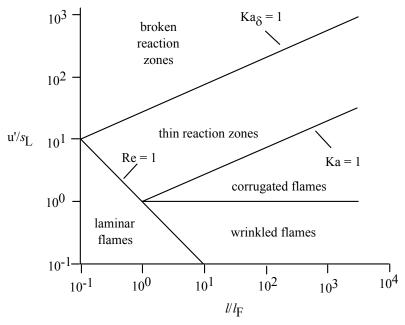

Figure 1. Regime diagram for premixed turbulent flames [1].

<w> is a local measure of combustion rate and a more global measure is required for characterization of combustion intensity. The burning velocity has traditionally been used for this measure despite the fact that it is an ill-defined quantity for both laminar and turbulent flames [4]. An unambiguous but difficult to determine measure of the global combustion rate is the burning rate integral, B_T, defined as the path integral of <w> across the flame brush [4]. The path is chosen to be perpendicular to <c> constant surfaces, a η path.

$$B_T \equiv \int_{-\infty}^{\infty} < w > d\eta. \quad (2)$$

It should be noted that in the case of steady, in the mean, planer flames with no imposed mean flow strain a burning velocity can be defined, and B_T divided by the reactant gas density equals that burning velocity.

For conditions under which Eq. (1) is valid, Eq. 2 can be expressed as follows.

$$B_T = \int_{-\infty}^{\infty} \rho_r S_L^0 I_0 \Sigma d\eta = \rho_r S_L^0 \int_{-\infty}^{\infty} I_0 \Sigma d\eta \quad (3)$$

In previous ARO sponsored research [5], it was shown that the surface density can be expressed as a function of the probability density function (PDF) of the reaction sheet

surface normal vector, $\underline{N}$, and of the reaction sheet crossing density along the η path, i.e., the average number of reaction sheet crossings per unit length of the path, n_c.

$$\Sigma = \left\langle \frac{1}{\lfloor \underline{N} \bullet \underline{n}_\eta \rfloor} \right\rangle_c n_c \quad (4)$$

In this expression, $\underline{n}_\eta$ is a unit vector defining the local orientation of the η path. The mean in Eq. 4 is evaluated from the PDF of $\underline{N}$; the subscript on the angle bracket denotes that the mean is weighted by the occurrence of a reaction sheet crossing the η path, crossing weighting. We have use crossed-plane tomography to measure the PDF of $\underline{N}$ and values of n_c and used these data to obtain Σ [6, 7].

Substituting (4) into (3) and manipulating one can show that

$$B_T = \rho_r S_L^0 \left\langle I_0 \left\langle \frac{1}{\lfloor \underline{N} \bullet \underline{n}_\eta \rfloor} \right\rangle_c \right\rangle_{FB} N_c \quad (5)$$

Here N_c is the path integral of n_c along η over the flame brush; it is the average number of times the reaction sheet crosses the η path. The subscript FB denotes that the mean is computed over all reaction sheet crossings of the η path. Models are needed for $<w>$, B_T and related quantities such as pollutant formation rates.

The measurements described in this report provide information on n_c, N_c, the PDF of $\underline{N}$ and on I_0 as revealed by temperature and temperature gradients – crossed-plane tomography and crossed-plane Rayleigh imaging. They can also give unique data for the magnitude of flow imposed reaction sheet/flamelet strain that affect the reaction sheet structure – combined crossed-plane tomography and stereo particle image velocimetry (SPIV). During the period of our grant we employed crossed-plane tomography, developed and employed crossed-plane Rayleigh imaging and demonstrated combined SPIV and crossed-plane tomography.

2. Summary of Results

Crossed-plane imaging measurements of surface normal vectors, $\underline{N}$: As noted, in previous research sponsored by ARO we developed and applied crossed-plane laser tomography to measure $\underline{N}$, its PDF, n_c, Σ and estimates of the burning rate of moderately wrinkled flames (I_0 = 1) in a series of V-flame studies [6, 8, 9, 10]. In addition crossed-plane acetone planar laser induced fluorescence measurements of flamelet normal vectors were made in a research spark ignition engine at the Combustion Research Facility, Sandia National Laboratories, Livermore, CA [7]. Measurements were made for three engine speeds at a fixed crank angle for each speed and under conditions for which the flamelet structure assumption is believed to be valid.

Two findings are common to all of our studies of $\underline{N}$ to date. The mean flamelet surface normal, $<\underline{N}>$, is perpendicular to the local mean progress variable, $<c>$, constant surface. When $\underline{N}$ is expressed in polar coordinates with polar angle ϕ and azimuthal angle θ defined with respect to a polar axis parallel to $<\underline{N}>$, its surface-weighted PDF has a common, single parameter form:

$$p_s(\phi,\theta)d\Omega = A\exp(-(\phi/\zeta)^2)\sin\phi d\phi d\theta \qquad (6)$$

ζ is the fit parameter that defines the distribution; A is the normalization constant and a function of ζ. The crossing weighted PDF needed to evaluate the average in Eq. 4 also has a common form:

$$p_c(\phi,\theta)d\Omega = B\exp(-(\phi/\zeta)^2)|\cos\chi|\sin\phi d\phi d\theta \qquad (7)$$

Here χ is the acute angle between $\underline{N}$ and η, the line crossed, and $|\cos\chi|$ is the magnitude of the dot product of $\underline{N}$ and a unit vector parallel to η. It is worth noting that in this case the dot product term in Eq. (4) varies nearly monotonically from one to two with increasing ζ [8]. Flamelet normal data along with crossing data have been used in the Eq. (5) to estimate the burning rate for the case of unperturbed flamelets, $I_0 = 1$, and good agreement with other measurements of the burning rate were observed [6]. Finally, we have used the assumption that Eq. 6 is valid to extract values of ζ from single plane tomography images as a function of position in V-flames [10]. We find that ζ increases nearly linearly with downstream distance from the base of the V.

At the beginning of our grant we used crossed-plane laser tomography to investigate differences in flamelet wrinkling associated with positive and negative Markstein number, Ma. Due to preferential diffusion effects positive Ma flames are stable, less susceptible to wrinkling, while negative Ma flames are unstable, more susceptible to wrinkling, than stable flames. In this study the breadth of the PDF of $\underline{N}$ was used as the measure of wrinkling and for the methane-air (Ma=-0.14) and ethylene-air (Ma=2.77) flames studied there was no significant difference in wrinkling.

Crossed-Plane Laser Rayleigh Imaging: A major achievement of our grant supported work is the development of crossed-plane Rayleigh imaging measurements of instantaneous isothermal surface normals, $\underline{N}_T$, and temperature gradient vectors. In premixed flames, elastic laser light scattering by molecules, Rayleigh scattering, is proportional to the molecular number density [13]. The constant of proportionality, the mixture average differential scattering cross-section, for methane– air flames is a weak function of reaction progress [14]. Assuming that this cross-section is independent of reaction progress, one can obtain from Rayleigh scattering images distributions of number density and, in turn, of temperature via the ideal gas law that relates number density, pressure and temperature (p=nkT). In addition, for unstretched flames Chemkin [11] based flame calculations of composition can be used to calculate the differential scattering cross-section as a function of temperature cross the flame [14]. Then the cross-section versus temperature relationship can be used to correct for cross section changes in finding number density and temperature[1]. The result, after correction, is an instantaneous snapshot of the 2-D temperature distribution.

From a snap shot, directional derivatives of temperature can be calculated for directions in the illumination plane. In crossed-plane Rayleigh imaging, snap shots of temperature in two orthogonal planes are obtained simultaneously with high energy, laser pulses. Along the line-of-intersection between the two illumination planes, directional derivatives in three orthogonal directions can be calculated giving thereby instantaneous temperature gradients along the line. In addition isothermal surface normal vectors can be determined and through repeated measurement its PDF and surface density can be determined [12].

---

[1] We have found it necessary to include depolarization effects for CO_2 and CO in the calculation of the scattering cross-section and would like to acknowledge the generous help of Campbell Carter of Wright Patterson Air Force Base.

To test the potential of Rayleigh imaging measurements on laminar methane-air (equivalence ratio, Φ, of 0.7) V-flames and a Bunsen flame have been made; measurements on a turbulent methane –air flame have also been made [12]. Typical laminar flame results are shown in Figure 2 where temperature profiles obtained in V- and Bunsen flames are compared to the temperature profile of an unstretched laminar flame calculated using the Chemkin package with GRImech chemistry [11]. The details of these measurements are outlined below. The main purpose of Figure 2 is to demonstrate our capability for obtaining temperature snapshots from Rayleigh imaging that have good agreement with laminar flame calculations.
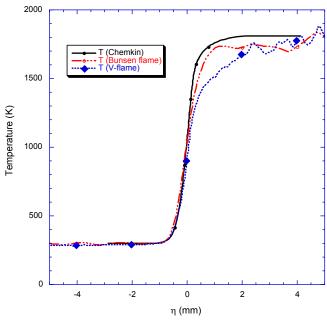

Figure 2. Comparisons of temperature profiles obtained from Rayleigh imaging temperature snap shots of laminar V- and Bunsen flames and from Chemkin based calculations.

The chief source of noise in the Rayleigh measurements is photon shot noise, which is proportional to the square root of the number density. Consequently the signal to noise ratio is lowest in high temperature regions. As evident from Figure 2 this noise is not significant at temperatures below approximately 1600 K. It is also evident from Figure 2 that the measurement system is able to resolve the thermal structure of the flame for temperatures up to about 1600 K. Above 1600 K there are differences between the measured profiles for the V-flame and the Bunsen flame and the calculated unstretched laminar flame profile. CO and CO_2 concentrations are relatively high in this regions and depolarization in CO and CO_2 scattering is important and must be accounted for. In addition since scattering levels are low background radiation is important. To account for background we have plans for estimating background levels in the product region and using this value to correct across the flame.

The apparatus used for crossed-plane Rayleigh scattering is shown schematically in Figure 3. Two intensified CCD (ICCD) cameras are used to record the light scattered from two orthogonal laser sheets. To avoid exposing the cameras to scattered light from both sheets, the cameras are exposed at different times and a delay loop in the optical path of one

laser beam is used to separate by approximately 20 ns the laser pulse arrival times of the two orthogonal sheets.
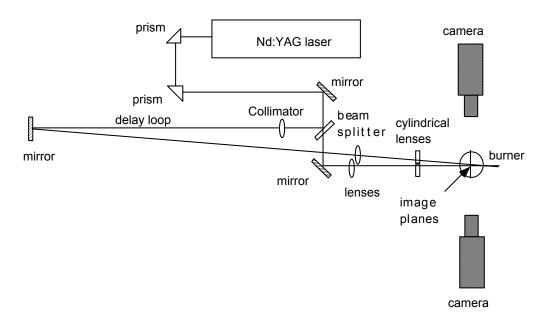

Figure 3. Schematic diagram of the apparatus used for crossed-plane Rayleigh scattering measurements. The laser source is a pulsed, frequency-doubled Nd: YAG laser with a pulse energy of approximately 200 mj. The temporal measurement resolution is set at approximately 20 nsec. by the time delay affected by the delay loop. The ICCD camera (512 x 512 pixels) exposure times are controlled by gating the intensifiers. The camera field of view is approximately 35 mm x 35 mm, and the spatial resolution of the measurements is better than 0.2 mm.

Crossed-plane Rayleigh measurements have been made in a Methane-Air flame and a sample of the results is shown in Figures 4 and 5.
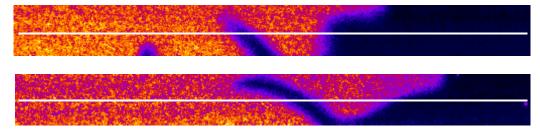

Figure 4. Crossed-plane Rayleigh temperature field images for a turbulent V-flame. Dark pixels indicate cold regions (reactants) and bright pixels indicate hot regions (products). The white lines indicate the position of the y-axis (measurement line).
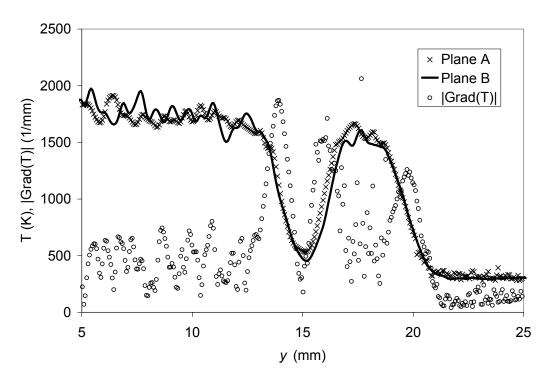
Figure 5. Temperature profile and $|\nabla T|$ data measured for the turbulent V-flame image pair shown in Fig. 4. The data are plotted against a spatial coordinate along the *y*-axis with an arbitrary origin. The temperature profiles, which are measured for the same line in space in two different imaging planes, are in good agreement. The $|\nabla T|$ data are well behaved for small *c*, but exhibit significant scatter for large *c*.

We have currently approximately 2000 turbulent flame image pairs from a methane-air (Φ=0.7) turbulent V-flame and are analyzing the data. The raw data and the preliminary temperature snap shot and gradient vector data obtained from them clearly demonstrate the feasibility and utility of crossed-plane Rayleigh imaging for thermal field studies. We expect to complete data analysis in a month or more and a manuscript reporting the work is in preparation [12].

Combined Stereo Particle Imaging Velocimetry and Crossed-Plane Tomography: SPIV allows one to measure a 2-D distribution of the 3-D velocity vector field. For SPIV, two CCD cameras, mounted in a Scheimpflug configuration, are focused from different angles onto the same plane. Each camera takes two exposures of scattering from seed particles in the flow at two closely spaced points in time and the displacements of the seed particles images between exposures is used to determine particle and thereby gas velocities. A single camera can be used to obtain the in plane velocity components; images from a pair of cameras allow one to estimate the out of plane velocity component as well as the in-plane components. A double-pulse, dual-head frequency doubled, 130 mj/pulse Nd: YAG laser fired sequentially in time is the light source for these measurements. The beams from the two laser heads are aligned colinearly and formed into overlapping sheets in the image plane of the cameras. The laser and image acquisition cameras are controlled by a data acquisition and analysis computer. A commercial SPIV system including lasers, optics, cameras and computer, purchased from

9

IDT with a DURIP grant from ARO, are being used for combined SPIV and crossed-plane tomography measurements.

The purpose of these measurements is to measure simultaneously the instantaneous reactant velocity field– by SPIV – in a vertical plane and the flamelet surface normal – by crossed-plane tomography - at points where the reactant velocity is also measured. A laser is used to illuminate two scattering planes oriented at 45º angles with respect to the vertical SPIV measurement plane. These two planes and the SPIV plane intersect along three horizontal lines, the measurement lines, and flamelet normal vectors are obtained where the flamelet intersects these lines. Two measurement lines are in the SPIV plane and where the flamelet intersects these lines we measure simultaneously $\underline{N}$ and the reactant velocity. These lines are marked a, b and c in Fig. 6b. A schematic of the apparatus used for the combined measurements is shown in Fig. 6a.

Measurements have been made on a methane-air flame with a bulk flow velocity of 2.17 m/s and a equivalence ratio of Φ=0.7. Turbulence was generated by a wire mesh grid positioned 50 mm upstream from the stabilizing rod. The grid has approximately 4.5 squares/cm^2, a 0.86 mm wire diameter, and a mesh spacing, M, of 4.2 mm. *u'*, the turbulence intensity, at the measurement location in cold flow was 0.12 m/s, as measured by hot wire anemometry. Approximately 1500 image sets (2 crossed plane tomographic images and 4 SPIV images per set) were acquired and saved for image processing. Data for surface normal and reactant velocity have been obtained. From these date we have extracted so far reactant velocity components normal and tangent to the instantaneous flamelet surface and the difference between these quantities obtained at two closely spaced points. PDF's of such quantities are shown in Figures 7 and 8.

These data are presented to indicate the progress we have made to date with combined SPIV and crossed-plane tomography and the data we can obtain. The most important capabilities of the method include flamelet normal and velocity vector measurements at two closely spaced points. In addition we expect to extract the flamelet displacement speed relative to the reactants. At this time we are working to develop our data analysis tools and plan to make measurements in flames of different fuels and air over a range of turbulence conditions in both V-flame and Bunsen flame burners. The capability to make such measurements is a very significant development.
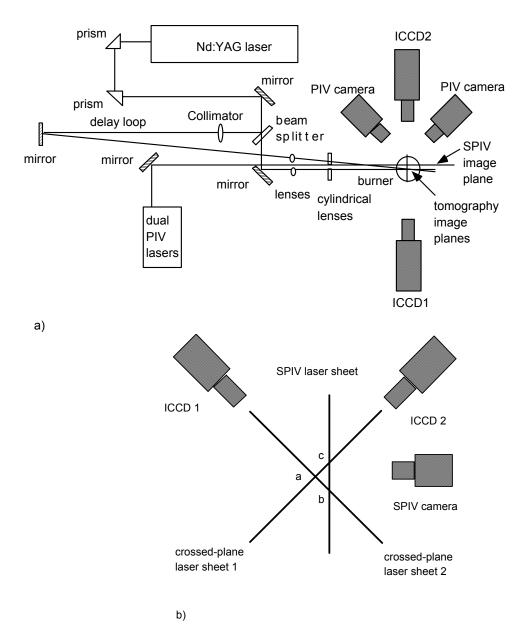
prism

Nd:YAG laser

ICCD2

prism

mirror

PIV camera

PIV camera

delay loop   Collimator

beam splitter

mirror

mirror

SPIV image plane

lenses   cylindrical lenses

burner

mirror

tomography image planes

dual PIV lasers

ICCD1

a)

ICCD 1

SPIV laser sheet

ICCD 2

c

a

b

SPIV camera

crossed-plane laser sheet 1

crossed-plane laser sheet 2

b)

Figure 6. Typical schematic diagrams of combined SPIV and crossed-plane laser tomography system. a) shows the overall layout of the system including lasers, cameras, optics and burner. b) shows the camera and laser sheet arrangement. The laser sheets propagate out of the plane of the paper. To avoid over-exposing the cameras to laser pulses, the SPIV images are taken first. The crossed-plane tomography images are taken a few tenths of a microsecond later. Surface normal vectors are measured where the 650 K isothermal surface crosses the three lines of intersection, denoted by a, b, and c, between the three illumination planes defined by laser sheets 1 and 2 and the SPIV laser sheet. Velocity vectors are obtained over the vertical SPIV laser sheet. The field of view of each of the four cameras is approximately 35mm x 35mm. The tomography cameras have 512 x 512 pixels, while the PIV cameras have 1360 x 1030 pixels.
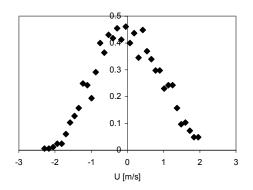
11

Figure 7a. PDF of reactant velocity component normal to the reaction sheet.
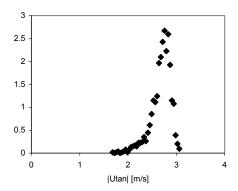

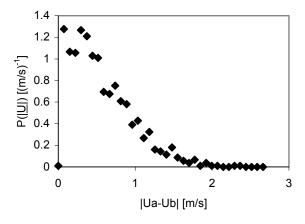**Figure 7b.** PDF of reactant velocity component tangent to the reaction sheet.

Figure 8. PDF of the magnitude of the difference of normal components of reactant velocity between the two SPIV measurement points.

3. Listing of Publications, Technical Reports, Presentations

a) Publications

D. A. Knaus, F. C. Gouldin, P. C Hinze and P. C. Miles, Measurement Of Instantaneous Flamelet Surface Normals And The Burning Rate In A SI Engine, *SAE Trans*. **108**, paper no. 1999-01-3543 (1999).

D. A. Knaus and F. C. Gouldin, Measurements Of Flamelet Orientations In Premixed Flames With Positive And Negative Markstein Numbers, *Proc. Comb Inst* **28**, 367 (2000).

D. A. Knaus, F. C. Gouldin and D. C. Bingham, Assessment Of Crossed-Plane Tomography For Flamelet Surface Normal Measurements, *Comb Sci. Tech* **174**, 101-134 (2002).

S. S. Sattler, F. C. Gouldin and D. A. Knaus, Determination Of Three- Dimensional Orientation Distributions In Turbulent V-Flames From Two-Dimensional Image Data, to appear in *Proc. Comb. Inst.* **29** (2002).

D. A. Knaus, F. C. Gouldin and S. S. Sattler, Crossed-Plane Rayleigh Imaging For Three - Dimensional Temperature Gradients In Premixed Turbulent Flamelets, *in preparation*.

b) Presentations
Invited Presentations:

Reacting Surface Structure in Turbulent Flames, F. C. Gouldin, AIAA 2003-0957, invited talk presented at the 41st Aerospace Sciences Meeting, January 2003, Reno, Nevada.

Premixed Turbulent Combustion: Flamelet Structure and Combustion Intensity, F. C. Gouldin, Invited Talk, 2001 Technical Meeting of the Eastern States Section of the Combustion Institute, Hilton Head, NC, December 2001.

Measurement Techniques for Turbulent Flames: From Time-Resolved Thermocouples to Flamelet Images, F. C. Gouldin, Invited Talk, ASME Heat Transfer Meeting, Pittsburgh, PA, August 1999.

Contributed Presentations:

Measurement of Instantaneous Flamelet Surface Normals and Burning Rate in a SI Engines, Knaus, Gouldin, Hinze and Miles, presented at the SAE International Fuels and Lubricants Meeting and Exposition, Toronto, Canada, Oct. 1999.

Flamelet Orientation and the Burning Rate Integral of SI Engine Flames, Knaus, Gouldin, Hinz, and Miles, presented at the Fall Technical Meeting of the Eastern States Section of the Combustion Institute, NC State, Raleigh, NC, October 1999.

Measurements Of Flamelet Orientations In Premixed Flames With Positive And Negative Markstein Numbers, D. A. Knaus and F. C. Gouldin, presented at the 28th Combustion Symposium, Edinburgh, Scotland, July 2000.

Measurements Of Three-Dimensional Flamelet Orientation Distributions Of Turbulent V-Flames At Various Axial Heights From Two-Dimensional Data, S. S. Sattler, D. A. Knaus, and F. C. Gouldin, presented at the 2nd Joint Meeting of the US Sections of the Combustion Institute, March 2001

Determination Of Three- Dimensional Orientation Distributions In Turbulent V-Flames From Two-Dimensional Image Data, S. S. Sattler, F. C. Gouldin and D. A. Knaus, presented at the 29th Combustion Symposium, Sapporo, Japan, and July 2002.

Crossed-Plane Rayleigh Imaging of Premixed Turbulent Flames, D. A. Knaus, S. S. Sattler, F. C. Gouldin, 29th Symposium poster presentation, Sapporo, Japan, July 2002.

c) Proceedings and Preprints:

Flamelet Orientation and the Burning Rate Integral of SI Engine Flames, Knaus, Gouldin, Hinz, and Miles, in the Proceeding of the Fall Technical Meeting of the Eastern States Section of the Combustion Institute, NC State, Raleigh, NC, October 1999.

Measurements Of Three-Dimensional Flamelet Orientation Distributions Of Turbulent V-Flames At Various Axial Heights From Two-Dimensional Data, S. S. Sattler, D. A. Knaus, and F. C. Gouldin in the Proceeding of the 2nd Joint Meeting of the US Sections of the Combustion Institute, March 2001.

Cycle-to-Cycle Variations and Burning Rate Estimates of SI Engine Flames Based on Flamelet Orientation Measurements, D. A. Knaus and F. C. Gouldin in Proceedings of 2nd Joint Meeting of the US Sections of the Combustion Institute, March 2001.

Premixed Turbulent Combustion: Flamelet Structure and Combustion Intensity, F. C. Gouldin in Proceedings of the 2001 Technical Meeting of the Eastern States Section of the Combustion Institute, Hilton Head, NC, December 2001.

Reacting Surface Structure in Turbulent Flames, F. C. Gouldin, AIAA 2003-0957, 41st Aerospace Sciences Meeting, January 2003, and Reno, Nevada.

4 Scientific Personnel

Darin A. Knaus, PhD, August 2002.

Sandra S. Sattler, PhD, expected June 2004.

5. Report of Inventions – none.

6. Bibliography

1. N. Peters, *Turbulent Combustion*, Cambridge (2000).

2. K.N.C. Bray and N. Peters, Laminar flamelets in turbulent flames, P.A. Libby and F.A. Williams, eds. *Turbulent Reacting Flows*, Academic Press, San Diego (1994).

3. D. Veynante and L. Vervisch, Turbulent combustion modeling, *Prog. Energy Comb. Sci.* **28**, 193-266 (2002).

4. F. C. Gouldin, Combustion intensity and burning rate integral of premixed flames, *Proc. Comb. Inst.* **26**, 381-388 (1996).

5. F. C. Gouldin, Analysis of certain algebraic closure models for premixed turbulent combustion, F. Dryer and R. Sawyer, eds, *Physical And Chemical Aspects Of Combustion: A Tribute To Irvin Glassman*, Gordon and Breach, Amsterdam (1997).

6. D. C. Bingham, F. C. Gouldin and D. A. Knaus, Crossed-plane laser tomography: Direct measurements of the flamelet surface normal, *Proc. Comb. Inst.* **27**, 77-84 (1998).

7. D. A. Knaus, F. C. Gouldin, P. C Hinze and P. C. Miles, Measurement of instantaneous flamelet surface normals and the burning rate in a SI engine, *SAE Trans.* **108**, paper no. 1999-01-3543 (1999).

8. D. A. Knaus, F. C. Gouldin and D. C. Bingham, Assessment of crossed-plane tomography for flamelet surface normal measurements, *Comb Sci. Tech* **174**, 101-134 (2002).

9. D. A. Knaus and F. C. Gouldin, Measurements of flamelet orientations in premixed flames with positive and negative Markstein numbers, *Proc. Comb Inst* **28**, 367 (2000).

10. S. S. Sattler, F. C. Gouldin and D. A. Knaus, Determination of three- dimensional orientation distributions in turbulent V-flames from two-dimensional image data, to appear in *Proc. Comb. Inst.* **29** (2002).

11. R. J. Kee, F. M. Rupley, J. A. Miller, M. E. Coltrin, J. F. Grcar, E. Meeks, H. K. Moffat, A. E. Lutz, G. Dixon-Lewis, M. D. Smooke, J. Warnatz, G. H. Evans, R. S. Larson, R. E. Mitchell, L. R. Petzold, W. C. Reynolds, M. Caracotsios, W. E. Stewart, P. Glarborg, C. Wang, and O. Adigun, CHEMKIN Collection, Release 3.6, Reaction Design, Inc., San Diego, CA (2000).

12. D. A. Knaus, S. S. Sattler and F. C. Gouldin, Crossed-plane Rayleigh Imaging for Three - Dimensional Temperature Gradients in Premixed Turbulent Flamelets, in preparation.

13. C. Eckbreth, *Laser Diagnostics For Combustion Temperature And Species*, Gordon and Breach, Amsterdam (1996).

14. F. C. Gouldin and R. N. Halthore, Rayleigh scattering for density measurements in premixed flames -- one point, time series data, *Exp. Fluids* **4**, 269-278 (1986).

REPORT DOCUMENTATION PAGE

Form Approved
OMB NO. 0704-0188

1. AGENCY USE ONLY (Leave Blank)	2. REPORT DATE 28 March 2003	3. REPORT TYPE AND DATES COVERED Final Progress 23 Aug 99 – 31 Dec 02

4. TITLE AND SUBTITLE
Crossed-Plane Imaging of Premixed Turbulent Combustion Processes

5. FUNDING NUMBERS
Grant #
DAAD 19-99-1-0324

6. AUTHOR(S)
F. C. Gouldin

7. PERFORMING ORGANIZATION NAME(S) AND ADDRESS(ES)
Cornell University
Day Hall
Ithaca, NY 14853

8. PERFORMING ORGANIZATION REPORT NUMBER
MAE 1-03 FCG

9. SPONSORING / MONITORING AGENCY NAME(S) AND ADDRESS(ES)

U. S. Army Research Office
P.O. Box 12211
Research Triangle Park, NC 27709-2211

10. SPONSORING / MONITORING AGENCY REPORT NUMBER

38966.2-EG

11. SUPPLEMENTARY NOTES
The views, opinions and/or findings contained in this report are those of the author(s) and should not be construed as an official Department of the Army position, policy or decision, unless so designated by other documentation.

12a. DISTRIBUTION / AVAILABILITY STATEMENT

Approved for public release; distribution unlimited.

12b. DISTRIBUTION CODE

13. ABSTRACT (Maximum 200 words)

During the last several years we have developed and applied advanced imaging methods – crossed-plane laser tomography and crossed-plane laser Rayleigh imaging -- for high-resolution studies of scalar fields in premixed combustion. Laser tomography with micron sized, silicone oil droplets marks 650 K isothermal surfaces, and we have used crossed-plane tomography to measure for the first time in three dimensions the instantaneous orientation of these surfaces and to determine the probability density function of the surface normal vector, a statistical measure of surface wrinkling. Rayleigh scattering from premixed flames can be used for temperature imaging, and we have developed crossed-plane Rayleigh imaging in order to measure with high-resolution instantaneous temperature fields, temperature gradient vectors and isothermal surface densities in premixed reacting flows. Most recently we have combined crossed-plane tomography with stereo particle image velocimetry to measure for the first time reactant flow velocities and the components of this velocity both perpendicular and tangent to the reaction sheet. In this report progress from the inception of Grant number DAAD 19-99-1-0324 is summarized, and relevant information regarding publications and participants in the research is presented.

14. SUBJECT TERMS
Turbulent combustion, crossed-plane imaging, flamelet normal, flamelet surface density

15. NUMBER OF PAGES
16

16. PRICE CODE

17. SECURITY CLASSIFICATION OR REPORT UNCLASSIFIED	18. SECURITY CLASSIFICATION ON THIS PAGE UNCLASSIFIED	19. SECURITY CLASSIFICATION OF ABSTRACT UNCLASSIFIED	20. LIMITATION OF ABSTRACT UL

NSN 7540-01-280-5500

Standard Form 298 (Rev.2-89)
Prescribed by ANSI Std. 239-18
298-102

Enclosure 1